Bioverse: Origins of Life

Martin Schlecker[1] and et al.

[1]*Steward Observatory, The University of Arizona, Tucson, AZ 85721, USA; schlecker@arizona.edu*

ABSTRACT

tbd.

1. INTRODUCTION

Introduce OOL, the importance of planetary contexts

2. ORIGINS OF LIFE SCENARIOS AND THEIR PREDICTIONS

Present widely discussed OOL scenarios and their predictions on exoplanet observables; derive testable hypotheses.

In this section, we present some of the most prominent origins of life scenarios and their observational predictions. We focus on the necessary environmental conditions for the processes and reactions inherent to each scenario, and aim to identify distinct observables that are accessible via present and near-future remote sensing techniques.

2.1. *Hydrothermal vents*

e.g., Russell+2010 ... The hydrothermal vents scenario requires a direct contact of an ocean and the planetary mantle/crust. This requirement is not met on an ocean world with large amounts of water, where the water pressure on the ocean floor is high enough to form high-pressure ices (Noack+2016).

see discussion in Kite & Ford 2018 Sect. 6.4

SR: The sealing away of the planetary interior from the ocean due to high-pressure ice layers is a common assumption for water world exoplanets (in addition to the references above, see e.g. Hu et al. 2021). I'm not convinced it is correct, because of relatively recent evidence showing the possibility of molecular assimitation into such ices and subsequent transport, e.g., https://iopscience.iop.org/article/10.1088/0004-637X/769/1/29/meta, https://iopscience.iop.org/article/10.3847/1538-4357/acb49a/meta, https://iopscience.iop.org/article/10.3847/1538-4357/aa5cfe/meta (I'm sure there are other workers in this area, this is just the group with which I am familiar). Exoplaneteers mostly uniformly accept this proposition, so it's not an unreasonable assumption if you want to run with it so long as its acknowledged and caveated reasonably; I'm just highlighting this for your attention so that you can make an informed decision.

Prediction: Planets with high-pressure ices do not show biosignatures.

2.2. *Subaerial ponds*

... By its nature, the subaerial ponds scenario relies on rock surfaces exposed to the planetary atmosphere. Water worlds that have their entire planetary surface covered with water contradict this requirement and do not allow for the wet-dry cycling inherent to this origin of life scenario. The competition of tectonic stress with gravitational crustal spreading (Melosh 2011) sets the maximum possible height of mountains, which in the solar system does not exceed $\sim 20\,\mathrm{km}$. Such mountains

will be permanently under water on water worlds. Another impediment to wet-dry cycles is tidal locking of the planet as it stalls stellar tide-induced water movement and diurnal irradiation variability.

Prediction: Biosignatures occur outside the tidal locking zone and at bulk densities consistent with exposed rock..

> SR: I'm not a priori sold that tidal locking means that no wet-dry cycles occur. you can still have cycling driven by transient changes in instellation due to flares, for example (e.g., https://iopscience.iop.org/article/10.3847/1538-4357/aadfd1/meta). Similarly, I wonder if 3D effects might not give rise to variability (https://iopscience.iop.org/article/10.3847/PSJ/acc9c4/meta). I argue that it is more robust to establish a correlation between biosignatures and planets which show evidence of continents/land. I think that Ty Robinson in our department has done some work in this area, his papers might be a good starting point. Other papers which look relevant (but with which I am not familiar, as this is not my area): https://academic.oup.com/mnras/article/511/1/440/6501216, https://academic.oup.com/mnras/article/495/1/1/5733176, https://iopscience.iop.org/article/10.3847/1538-3881/aad775/meta, https://iopscience.iop.org/article/10.3847/1538-3881/aaed3a/meta, https://iopscience.iop.org/article/10.3847/1538-3881/ab2df3/meta

2.3. *UV flux*

A major hypothesis in the origin of life is that UV light played a constructive role in getting life started on Earth (see Ranjan et al. 2016, 2017c; Rimmer et al. 2018; Rapf & Vaida 2016; Pascal et al. 2012; Green et al. 2021; and sources therein).

If UV light is required to get life started, then there is a minimum planetary UV flux requirement to have an inhabited world. This requirement is set by competitor thermal processes; if the photo-reaction does not move forward at a rate faster than the competitor thermal process(es), then the abiogenesis scenario cannot function. On the other hand, abundant UV light vastly in excess of this threshold does not increase the probability of abiogenesis, since once the UV photochemistry is no longer limiting, some other thermal process in the reaction network will be rate-limiting process instead. Therefore, a putative dependence of life on UV light is best encoded as a step function (see, e.g., Ranjan et al. 2017c; Rimmer et al. 2018; Rimmer, Ranjan & Rugheimer 2021).

One origin-of-life scenario has been refined to the point where the threshold flux has been measured. The cyanosulfidic scenario has been shown to require a mean flux of at least $F_{\mathrm{NUV,min}} = (6.8 \pm 3.6) \times 10^{10}\,\mathrm{photons\,cm^{-2}\,s^{-1}\,nm^{-1}}$ integrated from 200–280 nm at the surface in order to function (Rimmer et al. 2018; Rimmer et al. 2021 Astrobiology; Rimmer et al. 2023).

> SR: This is an interesting number, because it is below what was available on early Earth (so this scenario could have worked on early Earth) but until recently it was below what was thought to be available on habitable zone M-dwarf exoplanets. So it was thought that identification of biosignatures on M-dwarf planets could therefore falsify the cyanosulfidic scenario, with a potential caveat for transient UV from flares. Two recent developments have complicated the picture. First, Rimmer et al. 2018 had an error in their radiative transfer routines. Correcting for this error, early M-dwarfs and highly active M-dwarfs emit enough UV to meet the Rimmer et al. 2018 criterion (Ranjan et al. 2023). Second, a recent publication argues that /all/ estimates of M-dwarf UV are underestimates, and that late M-dwarf stars have similar emission to Sunlike stars (Rekhi et al. 2023). I suspect this is incorrect, because it contradicts a lot of work from e.g. the MUSCLES collaboration and the HAZMAT project, but it's worth keeping an eye on in case it is correct after all.

We use this threshold value as our baseline case.

Prediction: Past UV flux and the occurrence of biosignatures are correlated.

2.4. *Other Processes related to the Origins of Life*
2.4.1. *Planetary redox state and evolution*

The synthesis of prebiotic compounds requires moderately to highly reduced chemical environments (Kitadai & Maruyama 2018, Benner+2020, Sasselov+2020, Lichtenberg & Clement 2022). ... Surficial origins of life chemistries are dependent on
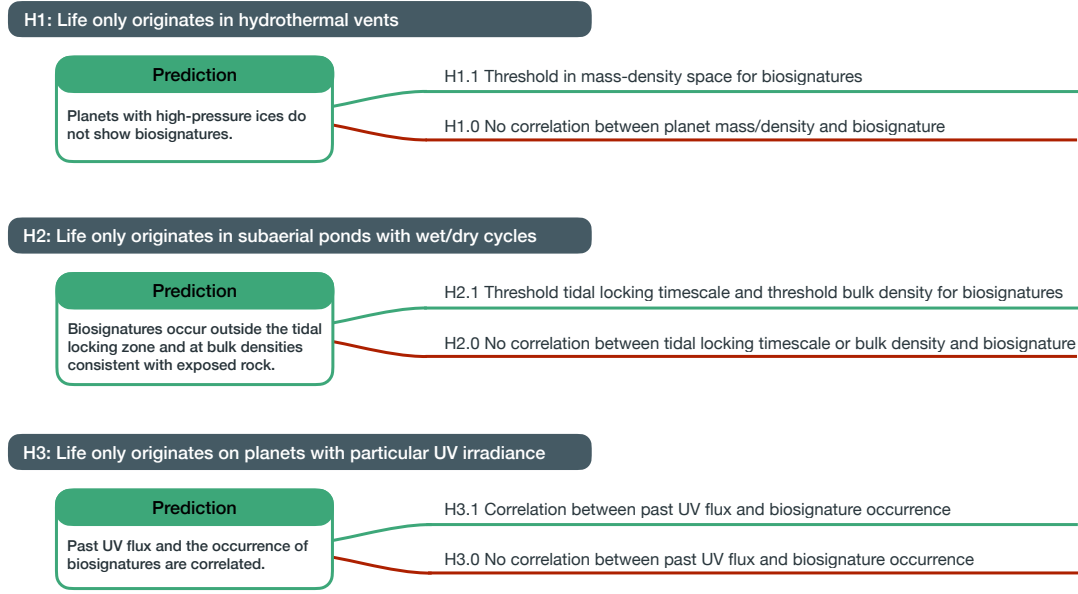
Figure 1. Origins of Life scenarios, their predictions on exoplanet observables, and derived population-level hypotheses.

the redox state of a planet being ~neutral (not too reduced or oxidized) to allow the presence of precursor molecules like HCN. The planetary redox state leaves an imprint on its atmospheric composition and thus planet size (very reduced atmospheres are large) and spectral signatures. Connected to the cyanosulfidic scenario, the pond scenario, and the impact trigger.

2.4.2. *Impact trigger*

Iron-rich impactors have been suggested to intermittently provide the reduced environments favored by prebiotic chemistry (e.g., Sekine+2003, Hashimoto+2007, Kuwahara & Sugita 2015, Genda+2017, Wogan+2023). ... Prebiotic synthesis triggered through reduced impactors that stochastically create transiently reducing or neutral atmospheres requires a certain composition of the impactors, the planet to not be in a magma ocean state (???) (Lichtenberg & Clement 2022), and, related to this requirement, occurrence of impact events during early planetary evolution. Suggested observables are stochastic increases in brightness temperature, transient increases of planet size, and change of planet composition (decreasing with decreasing impact rate, i.e., stellar age).

2.5. *Origins of Life Hypotheses*

... Figure 1 lists the hypotheses derived from the predictions of each OOL scenario. ...

3. METHODS

Briefly introduce Bayesian model comparison, then present the particular hypotheses in their mathematical form.

3.1. *Bayesian hypothesis testing with* `Bioverse`

3.2. *Considered planets and their orbits*

All Origins of Life scenarios considered here require water as a solvent; we thus consider only rocky planets that may sustain liquid water on their surface. Different formulations of habitable zones as regions around a star where a planet with Earth's atmospheric composition can maintain liquid water on its surface exist (e.g., Mol Lous et al. 2022; Spinelli et al. 2023; Tuchow & Wright 2023). CITE! Ramirez & Kaltenegger 2017, 2018 Here, we adopt the popular estimates of Kasting et al. (1993) and Kopparapu et al. (2013, 2014) that define a temperate zone between the runaway greenhouse transition CITE! and the maximum greenhouse limit CITE!. We use the parametrization in Kopparapu et al. (2014) to derive luminosity and planetary mass-dependent edges of the habitable zone (HZ) a_{inner} and a_{outer}. We further follow Bixel & Apai (2021) and classify as exo-Earth candidates (EEC) all planets with radii $0.8S^{0.25} < R < 1.4$ that orbit within the above boundaries. The lower limit was suggested as a minimum planet size to retain an atmosphere (Zahnle & Catling 2017).

3.3. *Exoplanet survey simulations*

biosignatures: Focus on molecular Oxygen? Excess Methane? (e.g., Seeburger et al. 2023)

A commonly discussed biosignature is molecular Oxygen (O_2), which on Earth emerged as a byproduct of photosynthesis during the Proterozoic era. No individual component of an atmosphere has been identified as a reliable biosignature in isolation (**?**), and the detection of Oxygen alone will certainly not be sufficient to confirm the presence of life. Nevertheless, we focus here on detecting this key absorber as it represents the general inherent observational challenges and trends.

3.3.1. *Habitable Worlds Observatory*

3.3.2. *Nautilus*

3.3.3. *LIFE*

3.4. *Fraction of inhabited planets with detectable biosignatures*

Presumably, not all habitable worlds are inhabited and not all inhabited worlds develop detectable biosignatures. The fraction of EECs that are both inhabited and harbor detectable biosignatures at the time when we observe them remains speculative; we aggregate them in the unitless parameter f_{life}.

3.5. *H1: Life only originates in hydrothermal vents*

The hydrothermal vent scenario does not allow oceans deep enough to form an impenetrable layer of high-pressure ice on its floor. The resulting allowed parameter space is described by a lower limit on the bulk density.

+ exclude atmospheric signature for water worlds?

...

3.6. *H2: Life only originates in subaerial ponds with wet/dry cycles*

We parametrize the required exposed land surface in this scenario as a lower limit in bulk density that is higher than for H1. Further, the tidal locking timescale of the planet may not be smaller than the age of the system. ...

3.7. *H3: Life only originates on planets with particular UV irradiance*

> Günther et al. (2020) relate U-band energy to bolometric flux.

> OPTIONAL: "We further test the scenario of a linear correlation of past UV flux and biosignature occurrence rate. This test requires the detection of multiple biosignatures."
> Test for negative correlations as well?

Our third theoretical experiment is to test the UV irradiance requirement (Sect. 2.3) by relating the occurrence of life on an exo-earth candidate with a minimum past quiescent stellar UV flux, focusing on the prebiotically interesting near-Ultraviolet (NUV) range from 200–280 nm.

> SUKRIT: got a good reference for this?

Our concrete hypothesis shall be that life only occurs on planets that at some point in their history have received such radiation exceeded a minimum flux $F_{\mathrm{NUV,min}}$.

3.7.1. *Semi-analytical analysis*

First, we apply a Bayes Factor Design Analysis (**?**) to assess the expected probabilities of obtaining true negative or true positive evidence for the hypothesis above, as well as the probability for misleading or inconclusive evidence.

Let our observable be the inferred past NUV flux of the planet F_{NUV}. Under Hypothesis H_3 (Equation 8), there exists a special unknown value of F_{NUV}, noted $F_{\mathrm{NUV,min}}$ such that

$$P(L|\theta, H_3) = f_{\mathrm{life}} \quad \text{if } \theta > F_{\mathrm{NUV,min}} \tag{1}$$

$$P(L|\theta, H_3) = 0 \quad \text{otherwise} \tag{2}$$

where f_{life} is the unknown probability of abiogenesis. The corresponding null hypothesis is that there exists no such special value of F_{NUV} and that

$$P(L|\theta, H_{3,\mathrm{null}}) = f_{\mathrm{life}}. \tag{3}$$

If we now define a sample of size n as $X = \{F_{\mathrm{NUV,i}}, L_i\}_{i \in [1,n]}$ where L_i is equal to 1 if life is detected and 0 otherwise, we can calculate the evidence for hypothesis H_i against H_j through the Bayes factor

$$BF_{H_i, H_j} = \frac{P(X|H_i)}{P(X|H_j)}, \tag{4}$$

with $P(X|H_i)$ and $P(X|H_j)$ likelihoods of obtaining the sample X under either hypothesis.

If we define $k = \sum L_i$ and denote Y the random variable that describes it, $H_{3,\mathrm{null}}$ represents the likelihood that the number of planets with life in the sample follows the binomial distribution

$$P(Y = k|H_{3,\mathrm{null}}) = \binom{n}{k} f_{\mathrm{life}}^k (1 - f_{\mathrm{life}})^{n-k}. \tag{5}$$

Under H_3, Y also follows a binomial distribution, however it is conditioned by $n_\lambda = Card(\{F_{\mathrm{NUV,i}} \text{ if } F_{\mathrm{NUV,i}} > F_{\mathrm{NUV,min}}\}_{i\in[1,n]})$ the number of values of F_{NUV} in the experiment that exceed $F_{\mathrm{NUV,min}}$

$$P(Y = k|H_3) = \binom{n_\lambda}{k} f_{\mathrm{life}}^k (1 - f_{\mathrm{life}})^{n_\lambda - k}. \tag{6}$$

Hence,

$$BF_{H_3, H_{3,\mathrm{null}}} = \frac{P(Y = k|H_3)}{P(Y = k|H_{3,\mathrm{null}})} = \frac{\binom{n_\lambda}{k}}{\binom{n}{k}} (1 - f_{\mathrm{life}})^{n_\lambda - n}. \tag{7}$$

Given a sample of planets, where for some of them we have convincing biosignature detections but remaining agnostic on f_{life}: What evidence for H_3 and $H_{3,\mathrm{null}}$ can we expect to get? Our Bayes factor (Equation 7) is determined by the unknown variables f_{life} and $F_{\mathrm{NUV,min}}$, as well as the number of planets with biosignature detections in the sample k. To compute the distribution of evidences, we repeatedly generated samples under H_3 and $H_{3,\mathrm{null}}$ and computed the Bayes factors $BF_{H_3, H_{3,\mathrm{null}}}$ and $BF_{H_{3,\mathrm{null}}, H_3}$. We then evaluated the fraction of Monte Carlo runs in which certain evidence thresholds (Jeffreys 1939) were exceeded.

3.7.2. *Survey simulations with Bioverse*

To model the sensitivity of the information gain of a proposed mission to sample selection and survey strategy, we now conduct survey simulations with Bioverse using different sample sizes and survey strategies. We again require that life occurs only on planets with sufficient past UV irradiation exceeding $F_{\mathrm{NUV,min}}$. Further, we require this flux to have lasted for a minimum duration ΔT_{min} to allow for a sufficient "origins timescale" (Rimmer 2023), and the planet to be within its momentary HZ during this entire period.

To determine HZ occupancy, we interpolated the stellar luminosity evolution grid of Baraffe et al. (1998) using a Clough Tocher interpolant (**??**, see left panel of Fig. 3) to compute the evolution of the inner (runaway greenhouse) and outer (maximum greenhouse) edges as a function of planet mass and stellar spectral type (Kopparapu et al. 2014). This provides each planet's epochs within and outside the HZ. For the NUV flux, we use the age- and stellar mass-dependent NUV fluxes in the HZ obtained by Richey-Yowell et al. (2023). We linearly interpolate in their measured grid, where we convert spectral type to stellar mass using the midpoints of their mass ranges ($0.75\,\mathrm{M_\odot}$ for K stars, $0.475\,\mathrm{M_\odot}$ for early-type M stars, and $0.215\,\mathrm{M_\odot}$ for late-type
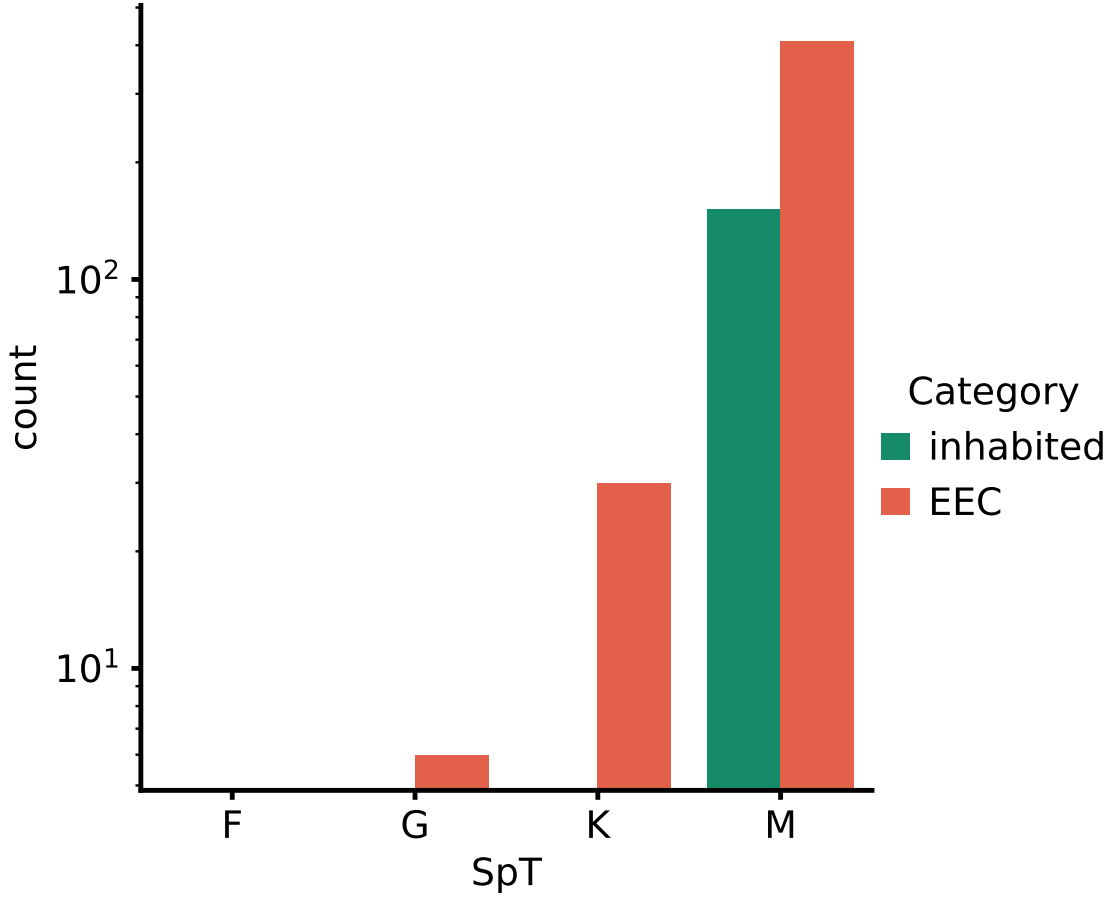
Figure 2. Host stars of all transiting planets, EECs, and inhabited planets. In a sample of 598 transiting planets, most EECs and all inhabited planets orbit M dwarfs.

M stars). Outside of the age and stellar mass range covered in Richey-Yowell et al. (2023), we extrapolate using nearest simplex (see right panel of Fig. 3).

We then determined which planets were both in the HZ and had NUV fluxes above $F_{\mathrm{NUV,min}}$ for $\Delta T_{\min} \geq 10\,\mathrm{Myr}$. We assigned the development of life to a random fraction f_{life} of all temperate planets fulfilling these requirements. For a population-level hypothesis, we then have

$$H_3 = f_{\mathrm{life}}(\theta, F_{\mathrm{NUV}}) = \begin{cases} 0, & F_{\mathrm{NUV}} < F_{\mathrm{NUV,min}} \\ f_{\mathrm{life}}, & F_{\mathrm{NUV}} \geq F_{\mathrm{NUV,min}} \text{ and in HZ for } \Delta t \geq 10\,\mathrm{Myr} \end{cases} \tag{8}$$
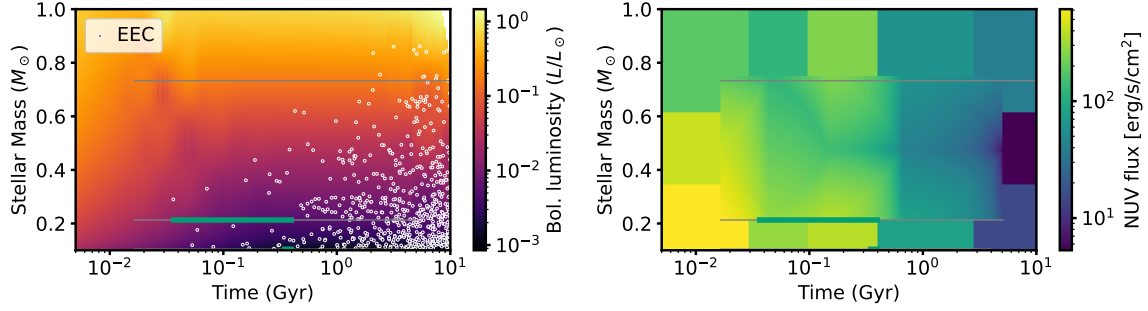
and the corresponding null hypothesis $H_{3,null} = f_{\mathrm{life}}(\theta)$, i.e., no correlation with UV flux.

As shown in Figure 2, the majority of EECs and all inhabited planets orbit M dwarfs.

4. RESULTS

4.1. *Information content in mass-density space*

4.2. *Information content in tidal locking timescale-density space*

Figure 3. Interpolated stellar luminosity evolution (left) and evolution of the NUV flux in the HZ as a function of host star mass. The scatter plot shows age and host star mass of the transiting planets in the synthetic sample with EEC highlighted in green. Two of the three planet trajectories shown have extended overlap of HZ occupancy and high NUV flux (green sections), our requirement for abiogenesis.
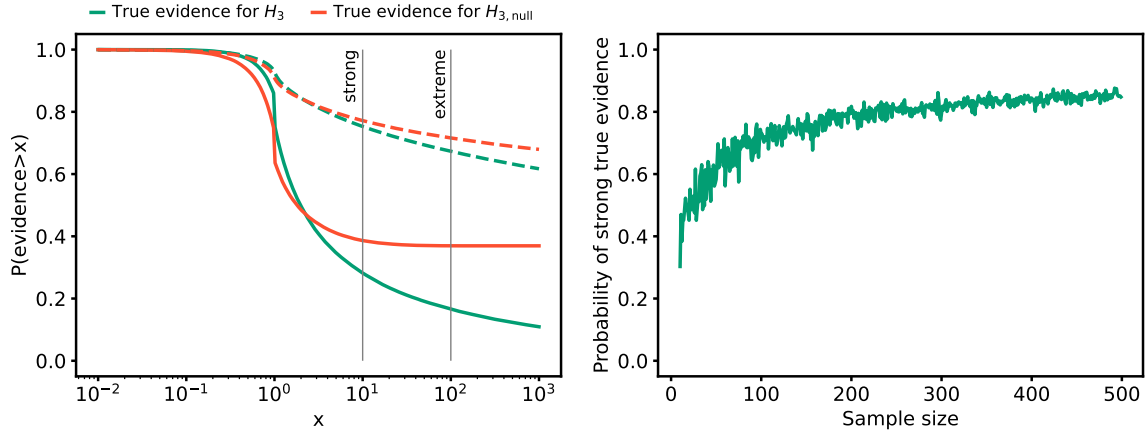
Figure 4. Probability to obtain true strong evidence. Left: evidence levels for H_3 and $H_{3,\text{null}}$ under sample sizes $n = 10$ (solid) and $n = 100$ (dashed). The vertical lines denote the thresholds for "strong" evidence, $BF_{H_i,H_j} > 10$, and "extreme" evidence, $BF_{H_i,H_j} > 100$. Right: Probability of true strong evidence for H_3 or $H_{3,\text{null}}$, whichever is smaller, as a function of sample size n.

4.3. *Correlation of past UV flux and biosignature occurrence*

4.3.1. *Semi-analytical approach*

In Section 3.7.1 we computed the probability for true positive evidence for H_3 and $H_{3,\text{null}}$ respectively. Figure 4 shows how these evidences are distributed for sample sizes 10 and 100, and how likely we are to obtain strong evidence ($BF_{H_i,H_j} > 10$). For $n = 10$, strong true evidence for H_3 ($H_{3,\text{null}}$) can be expected in $\sim 30\,\%$ ($\sim 40\,\%$) of all random experiments. In the majority of cases, the outcome of the survey will be inconclusive. The situation improves for larger samples – $80\,\%$ of random experiments yield true strong evidence under either H_3 or $H_{3,\text{null}}$.

The expected resulting evidence further depends on the a priori unknown abiogenesis rate f_{life} and on the NUV flux threshold. Figure 5 illustrates this dependency: For very low values of either parameter, samples drawn under the null or alternative hypotheses
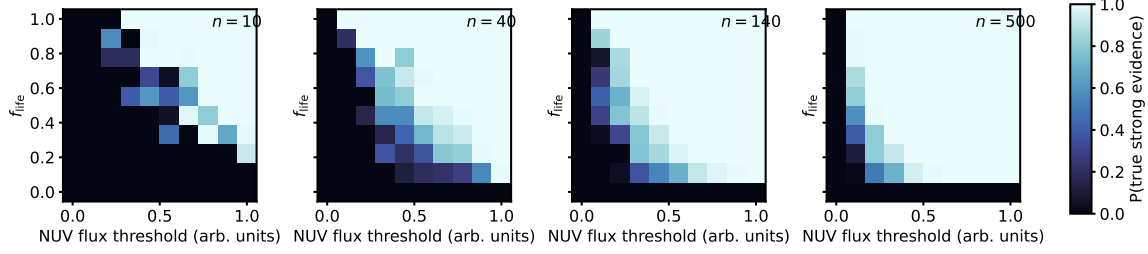
Figure 5. Probability of obtaining true strong evidence for different abiogenesis rates, NUV flux thresholds, and sample sizes. For each of these parameters, higher values increase the probability of yielding strong evidence.
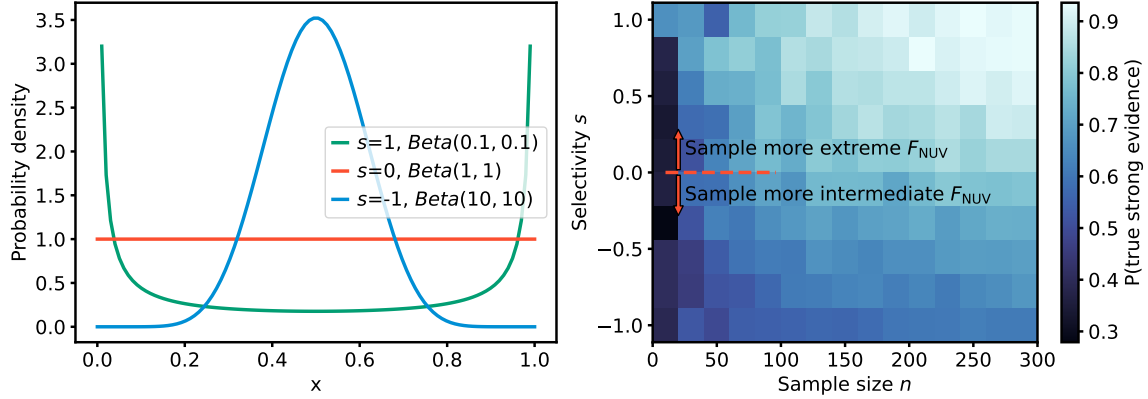

Figure 6. Scaling of the probability of obtaining true strong evidence with sample selectivity. Left: Sampling distribution for different selectivity parameters s. Right: Resulting P(true strong evidence). Sampling more extreme values of F_{NUV} is more likely to yield strong evidence.

are indistinguishable and the Bayesian evidence is always low. Both higher f_{life} and higher NUV flux thresholds increase the probability of obtaining strong evidence. Larger sample sizes enable this at lower values of these parameters.

So far, we have assumed random, uniform distributions of f_{life}, $F_{\mathrm{NUV,min}}$, and F_{NUV}. A high biosignature detection rate f_{life} increases the evidence (cmp. Equation 7) but we cannot influence it. The same is true for $F_{\mathrm{NUV,min}}$, where again higher values increase the evidence as the binomial distribution for H_3 gets increasingly skewed and shifted away from the one for $H_{3,\mathrm{null}}$. The distribution of F_{NUV} in the planet sample, on the other hand, can be influenced by the survey strategy. A targeted sampling approach could be to favor extreme values of F_{NUV} in the sample selection. Figure 6 shows how the probability of obtaining true strong evidence for H_3 scales with selectivity s, where $s \in]-1,1[$ such that $F_{\mathrm{NUV}} \sim Beta(1/10^s, 1/10^s)$. Here, $s = 0$ corresponds to a random uniform distribution. Compared to this case, a high selectivity can increase the probability of obtaining true strong evidence to $\gtrsim 85\,\%$ for large samples.

4.3.2. *Survey simulations with Bioverse*
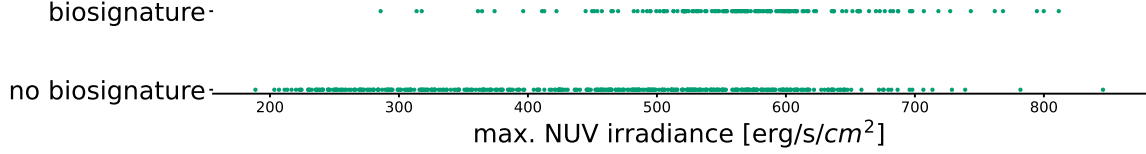
Figure 7. Recovered biosignature detections in the NUV flux – biosignature occurrence space. The dashed line denotes the threshold NUV flux $F_{\mathrm{NUV,min}}$.

In a magnitude- and volume-limited sample of a transit survey, the host star distribution will be skewed toward later spectral types and dominated by M dwarfs (see Fig. 2). Due to how the HZ scales with spectral type, by far most transiting EECs occur around M dwarfs. These host stars, in particular late subtypes, also provide extended periods of increased NUV emission that overlap with times when some of these planets occupy the HZ (see Fig. 3), our requirement for abiogenesis (compare Equation 8). Because of that, all inhabited planets orbit M dwarfs.

A representative recovery of the injected biosignature pattern is shown in Figure 7. There, we assumed an abiogenesis rate of $f_{\mathrm{life}} = 0.8$ and a minimum NUV flux of $F_{\mathrm{NUV,min}} = 350.0\,\mathrm{photons\,cm^{-2}\,s^{-1}\,nm^{-1}}$. This leads to a distribution of biosignature detections with detections increasingly occurring above a threshold inferred NUV flux.

We now investigate the sensitivity of the achieved statistical power of our default transit survey to the a priori unconstrained threshold NUV flux $F_{\mathrm{NUV,min}}$ and the abiogenesis rate f_{life}. Figure 8 shows the statistical power as a function of these parameters for a sample size of $N = 598$. Higher values of $F_{\mathrm{NUV,min}}$ increase the achieved statistical power of the survey, as the dataset under the alternative hypothesis H_3 differs more from the null hypothesis with increasing threshold flux. The same is true for the abiogenesis rate f_{life}, where higher values increase the evidence for H_3.

5. DISCUSSION

5.1. *What do we learn from a single biosignature detection?*

> discuss constraining power on OOL of a convincing biosignature detection on a single planet, depending on the position of the planet in the parameter space we explored.

5.2. *Constraining power for the origins of life as a function of biosignature location*

> How does the location of biosignature detections impact the credibility of OOL scenarios?

> biosignature on M dwarf planet vs. FGK: Impact on UV flux requirement?

5.2.1. *Sampling strategy for testing a predicted minimum NUV flux*

We show in Sect. 4.3 that the constraining power for testing the hypothesis of a minimum past NUV flux required for abiogenesis is sensitive on the occurrence of life, the value of this threshold flux, the sample size, and the distribution of sampled past NUV fluxes. In particular the last parameter offers an opportunity to optimize the survey strategy: Although constraints on a planet's UV history have generally large uncertainties (e.g., Richey-Yowell et al. 2023), the likely maximum flux of a planet
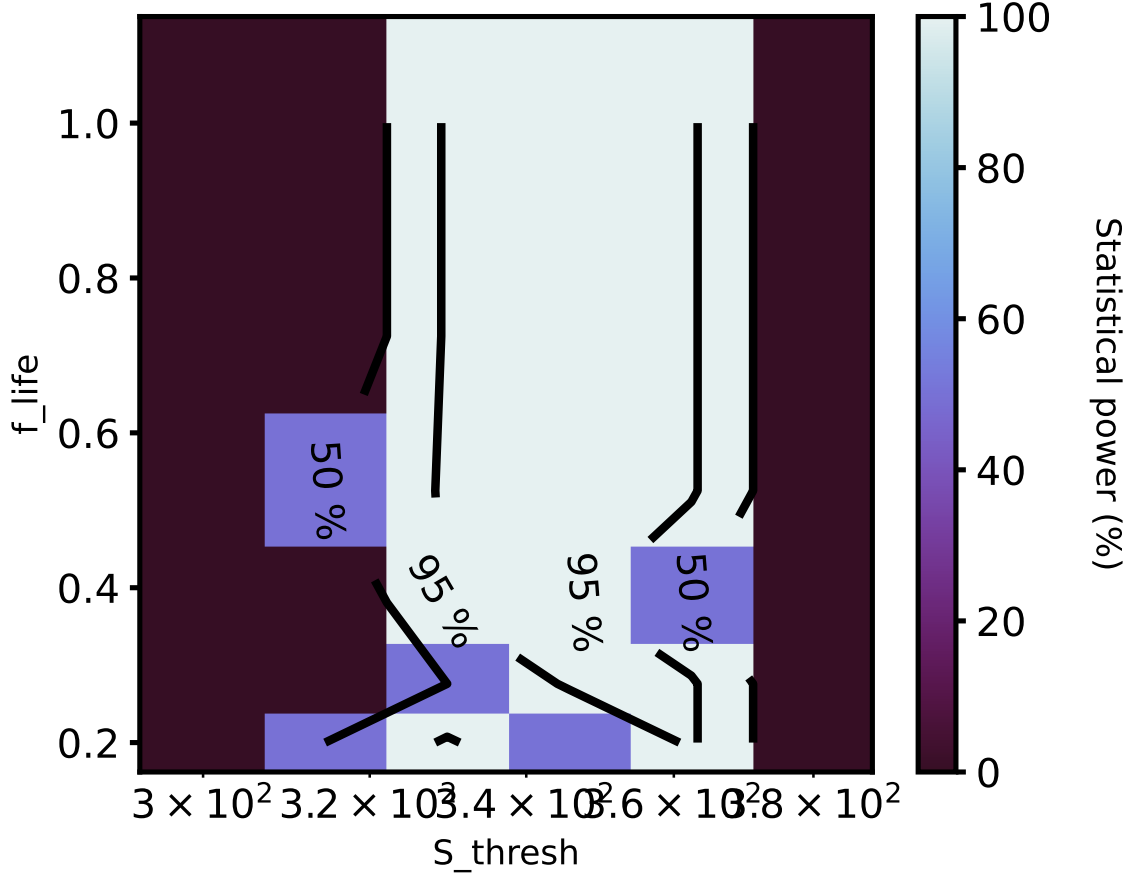
Figure 8. Statistical power as a function of threshold NUV flux and abiogenesis rate. For a given sample size (here: $N = 598$), the achieved statistical power of the survey is enhanced for higher values of $F_{\mathrm{NUV,min}}$ and f_{life}.

can be inferred and used as a proxy. Sampling more extreme (low and high) values for the maximum flux increases the probability of obtaining true strong evidence for the hypothesis. For large sample sizes $\gtrsim 200$, this strategy can push this probability into the 90 % range.

> and what about the probability of getting true strong evidence for H0?

5.3. *Contextual support for potential biosignature detections*

> discuss how planetary context may impact credibility of tentative biosignature detections (e.g., if there is a good fit with a predicted OOL pattern; or the opposite: the planetary context does not fit well to any OOL scenarios)

As we have shown in Section 4.3, the interplay of NUV evolution and HZ occupancy strongly favors late spectral types for abiogenesis via the cyanosulfidic scenario. This strong predicted correlation between stellar spectral type and the occurrence of life can be used to falsify Origins of Life (OoL) scenarios. The constraint of this context is particularly strong if a candidate biosignature is detected on a planet orbiting an earlier type star, i.e., where it is unexpected in the context of this OoL scenario.

5.4. *Caveats*

5.4.1. *Atmosphere transmission*

Theoretical work suggests that the atmosphere of prebiotic Earth was largely transparent at near-UV wavelengths with the only known source of attenuation being Rayleigh scattering (Ranjan & Sasselov 2017; Ranjan et al. 2017). We thus approximated surface UV flux using top-of-atmosphere fluxes. This represents a conservative approach, since any planet that fails to meet the irradiance criterion receives even lower near-UV radiation at its surface.

SUKRIT please specify as neccessary

5.4.2. *Stellar flares*

Our assumptions on past UV flux neglect the contribution of stellar flares, which may be hypothesized as an alternative source of UV light (Ranjan & Sasselov 2017). This concerns mainly ultracool dwarfs, due to their low quiescent emission and high pre-main sequence stellar activity (**??**). Recent work indicates that the majority of stars show inadequate activity levels for a sufficient contribution through flares (Glazier et al. 2020; Ducrot et al. 2020; Günther et al. 2020). The biosignature surveys we simulated here may test the hypothesis of sufficient UV radiation via stellar flares.

5.4.3. *Diurnal cycles*

We assume that tidal locking implies that there are no wet-dry cycles. Challenge this assumption.

6. CONCLUSIONS AND FUTURE WORK

Our main findings are:

1. Models of the Origins of Life provide hypotheses that are testable with near-future exoplanet surveys.

2. The required NUV radiation in the cyanosulfidic scenario should lead to a correlation between past NUV flux and current occurrence of biosignatures, both of which will soon be observationally accessible.

3. The required sample size for detecting this correlation depends on the occurrence of life on temperate exoplanets, the distribution of host star spectral types in the sample, ... A direct imaging mission with the Habitable Worlds Observatory (HWO) will require characterizing XXX planets ...

4. If the predicted NUV correlation exists, yielding strong evidence for it is likely ($> 90\,\%$) for sample sizes ≥ 100, and a survey strategy that targets extreme values of inferred past NUV irradiation.

5. Abiogenesis in the cyanosulfidic scenario strongly prefers late host star spectral types in a sample of transiting planets. Any potential biosignature detection on a planet around a star other than an M dwarf would disvafor this scenario and any other OoL theory requiring extended periods of high NUV irradiation.

REPRODUCIBILITY

REFERENCES

Baraffe, I., Chabrier, G., Allard, F., & Hauschildt, P. H. 1998, Astronomy and Astrophysics, v.337, p.403-412 (1998), 337, 403

Bixel, A., & Apai, D. 2021, The Astronomical Journal, 161, 228, doi: 10.3847/1538-3881/abe042

Ducrot, E., Gillon, M., Delrez, L., et al. 2020, A&A, 640, A112, doi: 10.1051/0004-6361/201937392

Glazier, A. L., Howard, W. S., Corbett, H., et al. 2020, ApJ, 900, 27, doi: 10.3847/1538-4357/aba4a6

Günther, M. N., Zhan, Z., Seager, S., et al. 2020, AJ, 159, 60, doi: 10.3847/1538-3881/ab5d3a

Jeffreys, H. 1939, Theory of Probability

Kasting, J. F., Whitmire, D. P., & Reynolds, R. T. 1993, Icarus, 101, 108, doi: 10.1006/icar.1993.1010

Kopparapu, R. K., Ramirez, R. M., SchottelKotte, J., et al. 2014, ApJL, 787, L29, doi: 10.1088/2041-8205/787/2/L29

Kopparapu, R. K., Ramirez, R., Kasting, J. F., et al. 2013, ApJ, 765, 131, doi: 10.1088/0004-637X/765/2/131

Mol Lous, M., Helled, R., & Mordasini, C. 2022, Nat Astron, 6, 819, doi: 10.1038/s41550-022-01699-8

Ranjan, S., & Sasselov, D. D. 2017, Astrobiology, 17, 169, doi: 10.1089/ast.2016.1519

Ranjan, S., Wordsworth, R., & Sasselov, D. D. 2017, Astrobiology, 17, 687, doi: 10.1089/ast.2016.1596

Richey-Yowell, T., Shkolnik, E. L., Schneider, A. C., et al. 2023, ApJ, 951, 44, doi: 10.3847/1538-4357/acd2dc

Rimmer, P. B. 2023, in Conflicting Models for the Origin of Life (John Wiley & Sons, Ltd), 407–424, doi: 10.1002/9781119555568.ch16

Seeburger, R., Higgins, P. M., Whiteford, N. P., & Cockell, C. S. 2023, Astrobiology, 23, 415, doi: 10.1089/ast.2022.0127

Spinelli, R., Borsa, F., Ghirlanda, G., Ghisellini, G., & Haardt, F. 2023, The Ultraviolet Habitable Zone of Exoplanets, doi: 10.48550/arXiv.2303.16229

Tuchow, N. W., & Wright, J. T. 2023, ApJ, 944, 71, doi: 10.3847/1538-4357/acb054

Zahnle, K. J., & Catling, D. C. 2017, ApJ, 843, 122, doi: 10.3847/1538-4357/aa7846